


# Growth of complex crystal on biopolymer surface: Synthesis and characterization

Polymers and Polymer Composites  
Volume 30: 1–7  
© The Author(s) 2022  
Article reuse guidelines:  
[sagepub.com/journals-permissions](https://sagepub.com/journals-permissions)  
DOI: 10.1177/09673911221089817  
[journals.sagepub.com/home/ppc](https://journals.sagepub.com/home/ppc)  


Leonardo Sobreira Rodrigues<sup>1</sup> , Adenilson Oliveira dos Santos<sup>2</sup>, Fernando Mendes<sup>3</sup>  and Ana Angélica Mathias Macêdo<sup>4</sup>

## Abstract

Although the physical properties of polymers already have been modified by changing different synthetic parameters, the effect of the crystallization by the doping is still rarely explored. In this work, a facile synthesis of composite chitosan film with copper L-valinate crystal (CHLVCu) was investigated. Composite films were prepared by the addition of copper II L-valine crystals (LVCu) in concentrations of 0.05, and 0.1 in 0.2% chitosan solution. The composite film of LVCu crystal dispersed in CH solution has been successfully obtained by the technique of solvent slow evaporation at low temperature. CHLVCu composite films are crystalline stabilizing the trans-LVCu phase. Homogeneity and low thermal stability have been proven by thermal measurements. The crystal growth takes place in the polymer surface. In addition, it is noteworthy that to the best of our knowledge, crystals complex of the LVCu has not been used as incorporate chitosan film and study has reported changes in physical properties composite film. The future this film can be application in area biomedical and technological.

## Keywords

Composite, chitosan, copper, crystalline, film

Received 19 January 2021; accepted 5 March 2022

## Introduction

Tissue engineering is an area that searches for new biocompatible materials that contribute to tissue reconstruction and replacement. The discovery of new products originated from natural sources will change the world market once they are accessible and are renewable, being strong market game-changers.<sup>1,2</sup>

Among the different materials available in nature, polymers have an increasing scientific interest, especially in the study of biopolymers, since they have special characteristics such as biodegradability and low toxicity.<sup>3,4</sup> These materials have big molecules (macromolecules) consisting of small units (monomers) that repeat themselves throughout the structure. The presence of polymers is evident in everyday life since their applicability involves several essential sectors, such as in the technological area.<sup>5,6</sup>

Chitin is the second most abundant biopolymer after cellulose in the world, being found in natural sources such as the exoskeleton of arthropods, and fungal cell walls.<sup>7</sup> Chitosan (CH) is obtained employing the alkaline deacetylation of chitin. Chitosan is a carbohydrate biopolymer classified as a semi-crystalline cationic copolymer composed of two monomeric  $\beta$  (1 $\rightarrow$ 4) linked units of N-acetyl-D-glucosamine and D-glucosamine.<sup>8</sup> The application of this polymer is wide, such as in agriculture,<sup>9</sup> biomedicine,<sup>10</sup> chemistry<sup>11</sup> and food products<sup>12</sup> among others. The capacity of this biopolymer is most evident associated with other materials, such as in polymer blends and metal ions, to promote synergistic properties.<sup>13–16</sup>

Copper is an essential mineral for living organisms where it performs important metabolic functions as in cell respiration, besides being essential to a variety of enzymatic processes. Many studies related to copper crystals complexes with amino

<sup>1</sup>CTEC, Universidade Federal de Alagoas, Maceió, Alagoas, Brazil

<sup>2</sup>CCSST, Universidade Federal do Maranhão, Imperatriz, Maranhão, Brazil

<sup>3</sup>Politécnico de Coimbra, ESTeSC, DCBL, Coimbra, Portugal

<sup>4</sup>LQM, Instituto Federal do Maranhão, Imperatriz, Maranhão, Brazil

## Corresponding author:

Leonardo Sobreira Rodrigues, CTEC, Universidade Federal de Alagoas, Av. Lourival Melo Mota, S/N, Tabuleiro do Martins, Maceio 57072-970, Brazil.  
Email: [sobreira.leon@gmail.com](mailto:sobreira.leon@gmail.com)



Creative Commons Non Commercial CC BY-NC: This article is distributed under the terms of the Creative Commons Attribution-NonCommercial 4.0 License (<https://creativecommons.org/licenses/by-nc/4.0/>) which permits non-commercial use, reproduction and distribution of the work without further permission provided the original work is attributed as specified on the SAGE and Open Access pages (<https://us.sagepub.com/en-us/nam/open-access-at-sage>).

acids are reported in the literature. The formation of the complex often stabilizes the reactivity of the metallic ion with other molecules. The stability of the complex contributes to increasing its use application wise, especially in the crystallization of these materials.<sup>17–21</sup>

In this wide range of complexes formed by copper and amino acids, there is the copper L-valinate crystal. This crystal has good stability; however, few properties have been explored yet.<sup>20</sup> Also, to our knowledge, its interaction with polymeric films is not known, and it is a potential product for many biomedical applications.

Crystallization from a solution involves two processes, the formation of the crystalline nucleus and the growth of the nucleus forming a stable solid crystalline lattice. The formation of single crystal allows to obtain a material with high purity, due to the crystalline arrangement making it difficult to insert impurities in the crystal structure.<sup>20,22</sup>

Currently, the growth of complex crystals on polymeric surfaces is still poorly discussed in the literature. Therefore, this study aims to synthesize a composite film formed by chitosan and copper L-valinate (CHLVCu) crystal as well as to study structural, vibrational and thermal properties for possible applications in bactericide and curative agents.

## Materials and methods

### Materials

L-Valine (98% purity), Chitosan (medium molecular weight) and  $\text{CuCl}_2 \cdot 2\text{H}_2\text{O}$  (99% purity) starting materials were obtained from the supplier (Sigma-Aldrich).

### Crystal growth

The crystal was synthesized by the slow solvent evaporation method, which consists of the formation of crystals by increasing the concentration of the reactants due to solvent evaporation. The ratios were calculated by simply taking 2 mols of L-Valine to 1 mol of copper chloride. The materials were initially solubilized in 20 mL of deionized water in distinct beakers under constant agitation, with a molar concentration of 0.2 mol/L of L-Valine and 0.1 mol/L of copper chloride. The copper solution was slowly added to the amino acid solution. Soon afterwards, the solution was adjusted to pH 8 using 1M NaOH standard solution. The solution was stirred for 24 h. After the stirring period, the solution was filtered and stored in a room at constant temperature (25°C) until the formation of the single crystal.

### Film production

The polysaccharide (2% w/w) was solubilized in acetic acid solution (10% w/v). CHLVCu films were obtained from the solubilization of copper L-Valinate crystal powder in chitosan solution containing equivalent concentrations of 0.05% (CHLVCu005) and 0.1% (CHLVCu01) of the crystal. The technique of solvent slow evaporation at low temperature has been used for moulding of the film when kept at 15°C.

### Characterizations

**X-ray diffraction.** To characterize the powdered samples, X-ray diffraction (XRD) data were collected with an Empyrean powder diffractometer  $\text{Cu K}\alpha$  ( $\lambda = 1.5418 \text{ \AA}$ ) operating at 40 kV/40 mA. The diffractograms were obtained in the angular range of 5–40° (2 $\theta$ ) with a step size of 0.02° and with a counting time of 2 s/step. The Rietveld refinement was used for structural characterization of cis-LVCu crystal via GSAS software.<sup>23</sup>

The crystallinity degree (Equation (1)) of the composite films was calculated based on the diffractograms by following mathematical relation

$$\% \text{ Crystallinity} = \frac{\text{Area of crystallinity peaks}}{\text{Area of all peaks}} \times 100 \quad (1)$$

**Fourier transform infrared analysis.** To obtain the transmission spectrum, ATR technique was used using the Smarti-Omni Sampler Nicolet iS10 spectrophotometer from Thermo Scientific brand. The spectra obtaining range was 4000–700  $\text{cm}^{-1}$  using 64 scans with a spectral resolution of 2  $\text{cm}^{-1}$ .

**Thermogravimetric–differential thermal analysis.** Thermogravimetric–Differential Thermal Analysis (TG/DTA) measurement was performed together on a Shimadzu DTG-60 thermogravimetric analyser. The thermal measurements followed the analysis standard in a nitrogen atmosphere of 100 mL/min, in a range from 293 to 950 K and heating rate 10 °C/min.

## Scanning electron microscopy

Surfaces were observed using a Shimadzu SS 550 Superscan scanning electron microscopy. The samples were coated with gold powder and observed under a magnification of 1000 times.

## Results and discussion

### X-ray diffraction

X-ray diffraction measurements were carried out to analyse the crystallinity of each film sample (Figure 1). The diffraction graphic was cropped for better data analysis. In the graphic, it is possible to observe the differences in the diffraction pattern of samples doped with a crystal of copper. LVCu powder exhibited crystalline character, where major characteristic crystalline peaks (at  $8.8^\circ$ ,  $15.3^\circ$ ,  $17.7^\circ$ ,  $18.7^\circ$  and  $20.8^\circ$ ). From the refinement of the data of *cis*-LVCu crystal, we have obtained R-Factor  $R_{wp} = 5.90\%$ ,  $R_p = 4.56\%$  and  $S = 1.78$  for the goodness of fit (Figure 1(b)). The samples crystallize in a monoclinic structure with a C2 space group containing four molecules ( $Z=4$ ) per unit cell. The lattice parameters obtained were  $a = 21.371(4)$ ,  $b = 9.565(2)$ ,  $c = 7.423(1)$  Å, and degree  $\beta = 108.752(3)^\circ$ .<sup>24</sup> The XRD pattern of CH film showed two peaks at  $2\theta=8.6^\circ$  and  $2\theta=11.8^\circ$  which were attributed to its hydrated semi-crystalline structure, whereas the broad peak around  $2\theta=18.5^\circ$  shows an amorphous structure of chitosan.<sup>25,26</sup>

As the crystal mix occurs in the composition of the CH film, the material tends to increase the crystallinity (Figure 1(c)), this behaviour is perceived from all the samples with the formation of the peaks at  $2\theta = 7.5^\circ$  and  $29.9^\circ$ . The formation of these peaks are related to the *trans*-LVCu crystalline phase,<sup>27</sup> such behaviour suggests that the *trans*-LVCu phase is more stable in the polymeric matrix. It suggests that the preference for the *trans*-LVCu phase is related to the disruption of the chitosan-derived amino group as it interferes with the insertion of water molecules into the LVCu crystal structure. Amino groups have a greater affinity for metal centres such as copper and are strong field binders when compared to water molecules.

### Fourier transform infrared spectroscopy

In Figure 2, we can observe the Fourier Transform Infrared (FT-IR) spectra for the crystalline films in the  $700\text{--}4000\text{ cm}^{-1}$  region. The bands were classified according to their vibrations. A strong vibration is perceived between  $3600\text{--}3000\text{ cm}^{-1}$  relative to the OH group stretch of water. Such a band loses intensity with increasing LVCu concentration. This can be justified by the predisposition of the *trans* phase, as observed in the XRD graph (Figure 1). Two bands observed at  $2924\text{ cm}^{-1}$  and  $2847\text{ cm}^{-1}$  are related to the deformation of the  $\text{CH}_3$  group.<sup>28</sup> The absorption band located at  $1738\text{ cm}^{-1}$  may be associated with the formation of carboxylic dimers through intermolecular interactions. The band located at  $1644\text{ cm}^{-1}$  refers to the C=O stretch, while the vibration at  $1600\text{ cm}^{-1}$  is related to the N-H stretching, both belonging to chitosan.<sup>28,29</sup>

With the addition of the copper ion, the main amine II-related changes are seen at  $1600\text{ cm}^{-1}$  and  $1644\text{ cm}^{-1}$ . This variation may indicate that these groups have coordinated with the copper atom. Also, the bands found at  $1069\text{ cm}^{-1}$  and  $1031\text{ cm}^{-1}$  belong to the chitosan glycosidic vibrations. The variation of the band at  $1069\text{ cm}^{-1}$  suggests the occurrence of a coordinated Cu cross-linking between different chitosan chains, in which the Cu ion acts as a bridge between amino groups of two separate polysaccharide chains.<sup>28</sup>

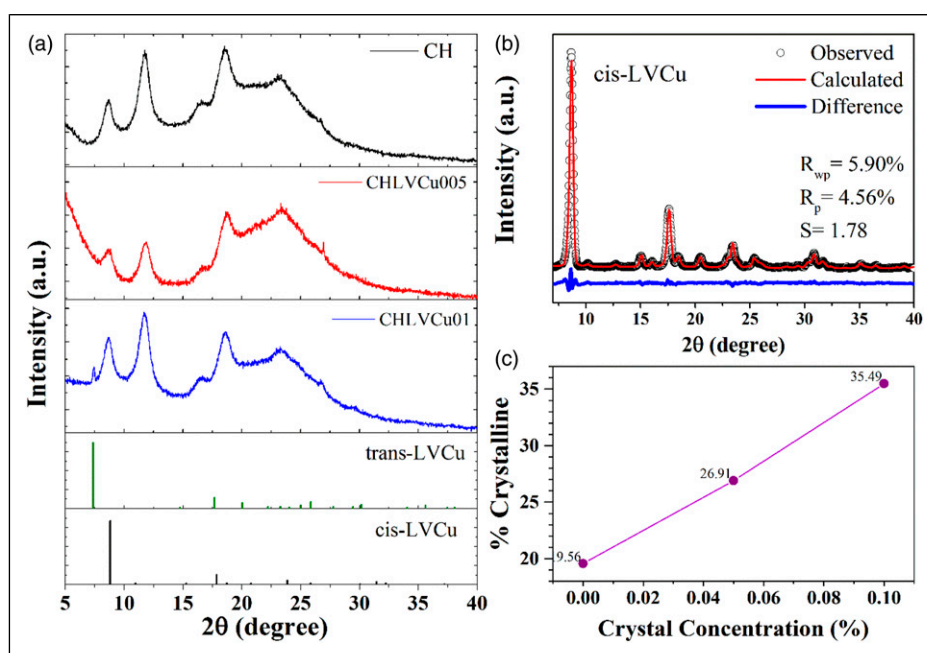


**Figure 1.** (a) X-ray diffraction pattern of CH, CHLVCu005, and CHLVCu01. (b) Rietveld refinement of XRD pattern of *cis*-LVCu crystal. (c) Crystalline percentage of films.

### Thermal analysis

Aiming to observe thermal properties of the synthesized materials, TG/DTA measurements were obtained. In Figure 3, we can observe the thermal characteristics of each film. All thermal processes are summarized in Table 1. For film, CH (Figure 3(a)) the observed mass loss equivalent to 15.13% is related to the endothermic event with a maximum point at 310 K. Such behaviour is related to the characteristic loss of water present in its structure. Subsequently, the material suffers several mass losses (83.81%) accompanied by three exothermic events. The degradation of the chitosan film starts at approximately 407 K, where the observed events are related to the degradation of organic compounds present in its structure. All films showed mass losses between 400 and 850 K representing the thermal decomposition of CH.<sup>30</sup> All other films showed three events of mass losses (Figures 3(b) and (c)).

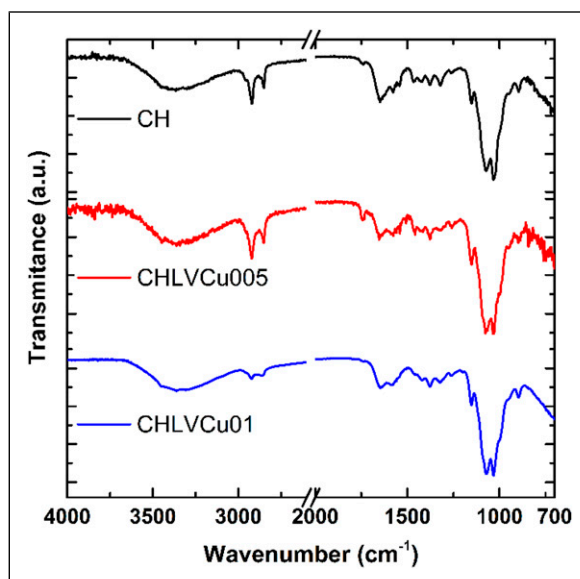


Figure 2. FT-IR spectrum of the CH, CHLVCu005 and CHLVCu01 composite films.

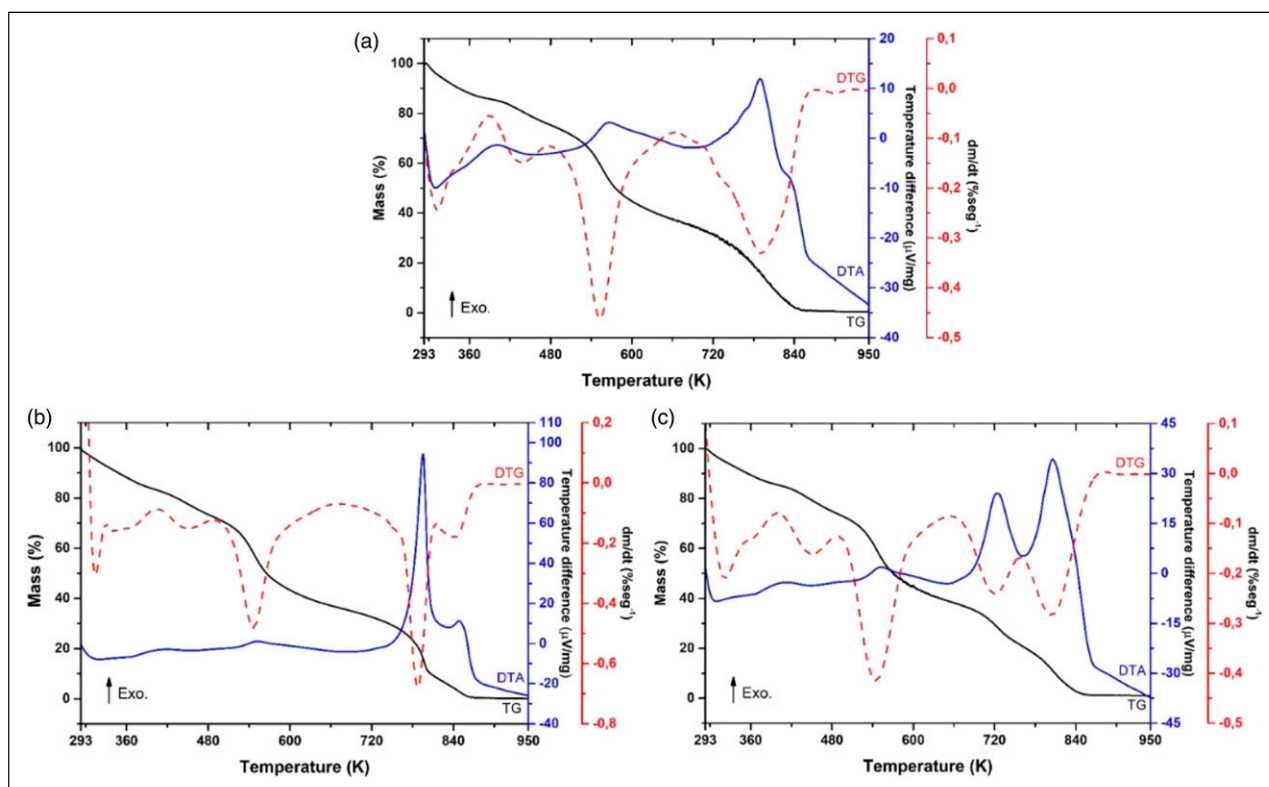


Figure 3. Thermograms of the (a) CH, (b) CHLVCu005 and (c) CHLVCu01 composite films.

The first is related to the loss of the water molecule between 295 and 480 K, which on average corresponds to 26% of the mass percentage, and could also be related to the volatilization of acetic acid trapped on the surface of the film.<sup>30</sup> The other two events between 490 and 880 K can be related to the break-up of chitosan chains, as well as the formation of secondary organic compounds such as amines, ketones and carbon dioxide. The degradation of chitosan and of amino acid is accompanied by exothermic peaks verified by DTA curves.

The incorporation of the LVCu crystal in the polymeric matrix structure does not significantly alter the thermal behaviour of the composite. As the degree of crystallinity of the material increases, as observed in the XRD graph (Figure 1), thermal curves tend to have more defined events. Thus, it can be proposed that the crystal was well dissolved in the structure of the CH matrix.

**Table 1.** Information regarding the thermal analyses of TG-DTA for CH, CHLVCu005 and CHLVCu01 composite films.

CH(LVCu) film (%)	TG/DTG			DTA (K)	Fragment
	T <sub>s</sub> (K)	T <sub>e</sub> (K)	Mass (%)		
0	297	406	15.13	310 <sub>(endo.)</sub>	H <sub>2</sub> O
	407	526	16.14	401 <sub>(exo.)</sub>	Organic compounds
	528	705	34.95	567 <sub>(exo.)</sub>	
	706	853	32.72	788 <sub>(exo.)</sub>	
005	295	496	27.52	319 <sub>(endo.)</sub> ; 416 <sub>(exo.)</sub>	H <sub>2</sub> O
	497	696	36.78	552 <sub>(exo.)</sub>	Organic compounds
	697	882	34.15	795; 848 <sub>(exo.)</sub>	
01	296	490	25.94	309 <sub>(endo.)</sub> ; 413 <sub>(exo.)</sub>	H <sub>2</sub> O
	491	654	34.65	552 <sub>(exo.)</sub>	Organic compounds
	654	871	37.39	723; 805 <sub>(exo.)</sub>	

DTA: Differential Thermal Analysis; end: Endothermic; exo: Exothermic; TG/DTG: Thermogravimetric/Derivative Thermogravimetric.

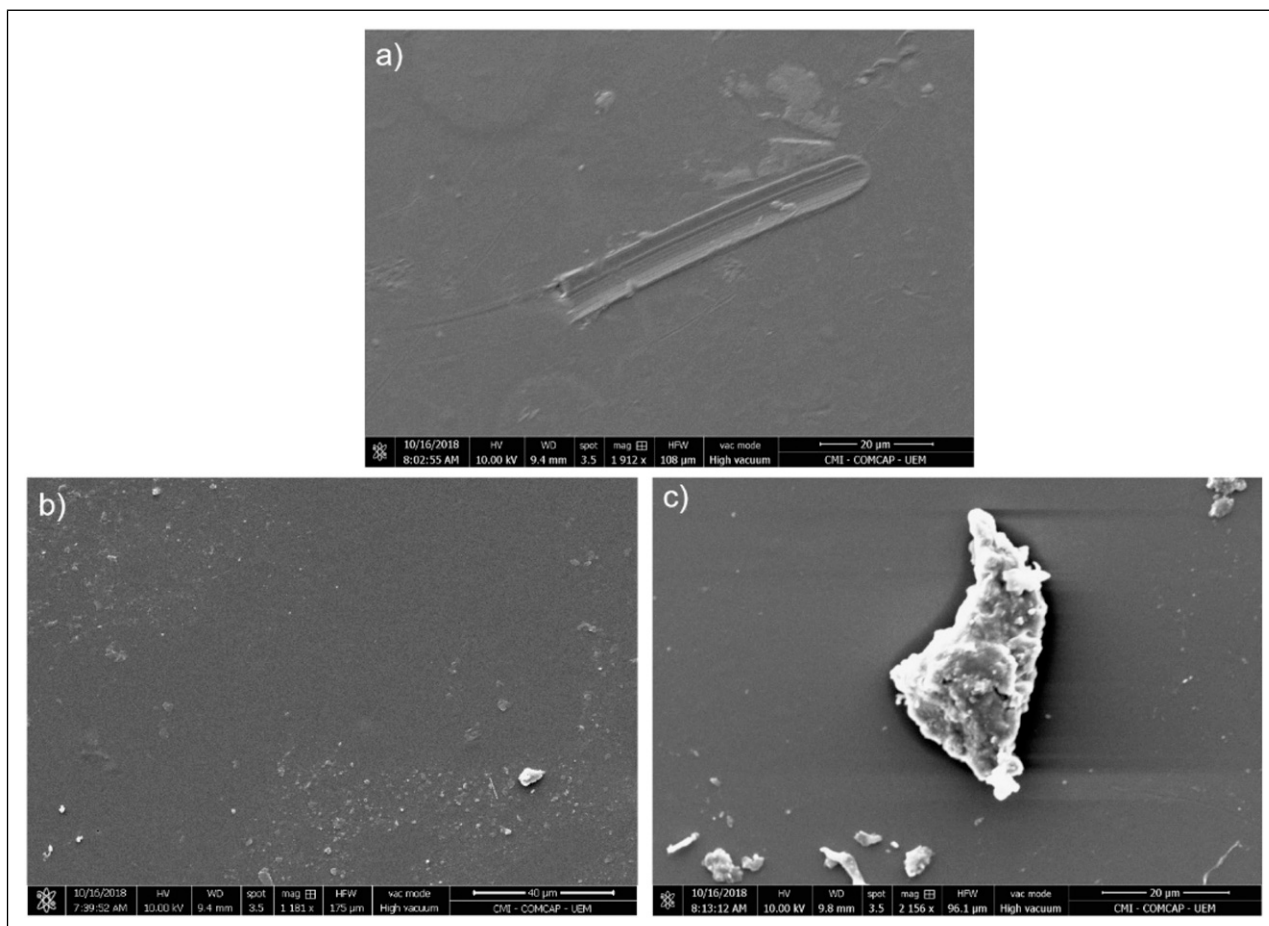


**Figure 4.** SEM image showing the surface of (a) CH, (b) CHLVCu005 and (c) CHLVCu01 composite films.

## Scanning electron microscopy

The surface morphology of chitosan-based films was investigated using scanning electron microscopy (SEM). Figure 4 shows the SEM images of CH and chitosan-based composite with loading three crystal LVCu concentrations (0.05 and 0.1% w/w). As shown in Figure 4 (a), the surface of pure CH film is rather smooth, compact and homogenous. In composite films (Figures 4(b) and (c)), crystal incorporation modified the CH surface, where the presence of small crystallites can be observed. Increasing the concentration of LVCu in the polymer matrix is expected to cause more crystals to appear on its surfaces.

## Conclusion

The composite film of LVCu crystal dispersed in CH solution has been successfully obtained by the technique of solvent slow evaporation at low temperature. It was observed that the composite film increases the crystallinity and homogeneity, with the trans-LVCu phase stabilized. These properties will contribute to the understanding of these composite films, in addition to enabling a future application in the biomedical and technological areas.

## Acknowledgements

We are grateful to the Complexo de Centrais de Apoio à Pesquisa (CONCAP) of the State University of Maringá (UEM) for providing the equipment (SEM) used in this investigation, to the Brazilian agencies.

## Declaration of conflicting interests

The author(s) declared no potential conflicts of interest with respect to the research, authorship, and/or publication of this article.

## Funding

The author(s) disclosed receipt of the following financial support for the research, authorship, and/or publication of this article: This work was supported by the Conselho Nacional de Desenvolvimento Científico e Tecnológico (CNPq), Coordenação de Aperfeiçoamento de Pessoal de Nível Superior (Capes), and Fundação de Amparo à Pesquisa e ao Desenvolvimento Científico e Tecnológico do Maranhão (FAPEMA) for financial support.

## ORCID iDs

Leonardo Sobreira Rodrigues  <https://orcid.org/0000-0002-1547-3420>

Fernando Mendes  <https://orcid.org/0000-0002-5205-8939>

## References

1. Chen F-M and Liu X. Advancing biomaterials of human origin for tissue engineering. *Prog Polym Sci* 2016; 53: 86–168.
2. Khademhosseini A and Langer R. A decade of progress in tissue engineering. *Nat Protoc* 2016; 11: 1775–1781.
3. Hoch E, Tovar GEM and Borchers K. Biopolymer-based hydrogels for cartilage tissue engineering. *Bioinspired, Biomim Nano-biomater* 2016; 5: 51–66.
4. Gsib O, Egles C and Bencherif SA. Fibrin: An underrated biopolymer for skin tissue engineering. *J Mol Biol Biotechnol* 2017; 2: 1–4.
5. Park S-B, Lih E, Park K-S, et al. Biopolymer-based functional composites for medical applications. *Prog Polym Sci* 2017; 68: 77–105.
6. Zhao S, Malfait WJ, Guerrero-Alburquerque N, et al. Biopolymer aerogels and foams: chemistry, properties, and applications. *Angew Chem Int Ed* 2018; 57: 7580–7608.
7. Kaur S and Dhillon GS. Recent trends in biological extraction of chitin from marine shell wastes: a review. *Crit Rev Biotechnol* 2015; 35: 44–61.
8. Gonçalves FJ and Freitas RP. Modification of chitosan by Zincke reaction: Synthesis of a novel polycationic chitosan-pyridinium derivative. *J Braz Chem Soc* 2019; 30: 2318–2323.
9. Gabriel Paulraj M, Ignacimuthu S, Gandhi MR, et al. Comparative studies of tripolyphosphate and glutaraldehyde cross-linked chitosan-botanical pesticide nanoparticles and their agricultural applications. *Int J Biol Macromol* 2017; 104: 1813–1819.
10. Pellá MCG, Lima-Tenório MK, Tenório-Neto ET, et al. Chitosan-based hydrogels: From preparation to biomedical applications. *Carbohydr Polym* 2018; 196: 233–245.
11. Huang R, Liu Q, Huo J, et al. Adsorption of methyl orange onto protonated cross-linked chitosan. *Arabian J Chem* 2017; 10: 24–32.
12. Zhang X, Xiao G, Wang Y, et al. Preparation of chitosan-TiO<sub>2</sub> composite film with efficient antimicrobial activities under visible light for food packaging applications. *Carbohydr Polym* 2017; 169: 101–107.
13. Liu Y, Cai Y, Jiang X, et al. Molecular interactions, characterization and antimicrobial activity of curcumin-chitosan blend films. *Food Hydrocoll* 2016; 52: 564–572.
14. Gopi S, Pius A, Kargl R, et al. Fabrication of cellulose acetate/chitosan blend films as efficient adsorbent for anionic water pollutants. *Polym Bull* 2019; 76: 1557–1571.
15. Frantz TS, Silveira N, Quadro MS, et al. Cu(II) adsorption from copper mine water by chitosan films and the matrix effects. *Environ Sci Pollut Res* 2017; 24: 5908–5917.
16. Pramanik A, Laha D, Dash SK, et al. An in-vivo study for targeted delivery of copper-organic complex to breast cancer using chitosan polymer nanoparticles. *Mater Sci Eng C* 2016; 68: 327–337.

17. Campbell MK and Farrell SO. *Biochemistry*. 7th ed. Florence, KY, USA: Cengage Learning, 2011.
18. Nelson DL and Cox MM. *Lehninger Principles of Biochemistry*. 7th ed. New York, NY: W. H. Freeman, 2017.
19. Dwyer DS. *Wiley Encyclopedia of Chemical Biology*. Hoboken, NJ, USA: John Wiley & Sons, Inc., 2008.
20. Fleck M and Petrosyan AM. *Salts of Amino Acids*. Cham, Switzerland: Springer International Publishing, 2014.
21. Oliveira Neto JG, Cavalcante LA, Gomes ES, et al. Crystalline films of l-threonine complexed with copper (ii) dispersed in a galactomannan solution: a structural, vibrational, and thermal study. *Polym Eng Sci* 2020; 60: 71–77.
22. Mullin JW. *Crystallization*. 4th ed. Butterworths, London: Elsevier, 2001.
23. Toby BH. EXPGUI, a graphical user interface for GSAS. *J Appl Crystallogr* 2001; 34: 210–213.
24. Steren CA, Calvo R, Castellano EE, et al. Molecular structure and single crystal EPR spectra of bis(L-Valinato)copper(II) monohydrate, Cu[H<sub>2</sub>NCH(CH<sub>3</sub>)<sub>2</sub>CHCO<sub>2</sub>]<sub>2</sub>·H<sub>2</sub>O. *Physica B: Condensed Matter* 1990; 164: 323–330.
25. Qin Y, Liu Y, Yuan L, et al. Preparation and characterization of antioxidant, antimicrobial and pH-sensitive films based on chitosan, silver nanoparticles and purple corn extract. *Food Hydrocoll* 2019; 96: 102–111.
26. Salari M, Sowti Khiabani M, Rezaei Mokarram R, et al. Development and evaluation of chitosan based active nanocomposite films containing bacterial cellulose nanocrystals and silver nanoparticles. *Food Hydrocoll* 2018; 84: 414–423.
27. Marković M, Judaš N and Sabolović J. Combined experimental and computational study of cis-trans isomerism in bis(L-valinato) copper(II). *Inorg Chem* 2011; 50: 3632–3644.
28. Qu J, Hu Q, Shen K, et al. The preparation and characterization of chitosan rods modified with Fe<sup>3+</sup> by a chelation mechanism. *Carbohydr Res* 2011; 346: 822–827.
29. Gritsch L, Lovell C, Goldmann WH, et al. Fabrication and characterization of copper(II)-chitosan complexes as antibiotic-free antibacterial biomaterial. *Carbohydr Polym* 2018; 179: 370–378.
30. Koosha M and Hamed S. Intelligent Chitosan/PVA nanocomposite films containing black carrot anthocyanin and bentonite nanoclays with improved mechanical, thermal and antibacterial properties. *Prog Org Coat* 2019; 127: 338–347.